

Studies of the Fragment-ion Distribution and Reaction with a Charge Spectrometer. VI. A New Interpretation of the Fragmentation Mechanism in CH_3X Based on the Molecular Orbital Method. (2)*

Shigeru IKUTA, Kenji YOSHIHARA, and Takanobu SHIOKAWA

Department of Chemistry, Faculty of Science, Tohoku University, Aoba, Aramaki, Sendai 980

(Received September 6, 1974)

We have proposed a new fragmentation mechanism and successfully applied it to various monosubstituted alkanes RX . The fragmentation mechanism can be described as follows: (1) The bond scission first occurs where the electrons exist densely in the particular occupied molecular orbital correlated to the particular ionization. (2) Process (1) competes with the electron redistribution. (3) In the higher-energy region, secondary scission also occurs. The breakdown curves of the CH_3NH_2^+ , CH_3SH^+ , and CH_3Br^+ produced by charge-exchange reactions have been obtained by the use of a perpendicular double-mass spectrometer. The experimental results can be satisfactorily explained by the proposed mechanism on the basis of the calculated eigenvectors of the various molecular orbitals.

The fragmentation mechanism of molecules by electron or photon impact has usually been interpreted by the quasiequilibrium theory (QET) first proposed by Rosenstock *et al.*¹⁾ and later improved by other researchers.²⁾ Nevertheless, this theory does not have a wide applicability, especially in cases of very large and very small molecules.^{3,4)}

Hirota⁵⁾ and Lorquet⁶⁾ have suggested that the scission probability of the skeletal bonds is proportional to the electron densities of the highest occupied molecular orbital at the corresponding bond. However, this theory cannot completely explain the energy dependence of the mass spectra, as was pointed out in a previous paper.⁷⁾ Furthermore, in the cases of molecules with lone-pair electrons, the highest occupied MO is non-bonding, and the ionization caused by the loss of the non-bonding electron results in the formation of the stable molecular ion and does not result in the formation of the fragment ions. Therefore, in these molecules, Hirota's proposal is incomplete as an explanation of the production of the fragment ions.

In a previous paper⁸⁾ on the breakdown curves of various CH_3X substances ($\text{X}=\text{NH}_2$, OH , SH , Cl , Br , and I), we found that the C-X bond in methyl halides (Group A) easily dissociates, while that in methylamine, methanol, or methyl mercaptan (Group B) does not. This difference can be interpreted in terms of the main character of the various occupied MO's calculated by the Extended Hückel Molecular Orbital method,⁹⁾ on the assumption that fragmentation occurs at the bond at which an electron is ejected.

In this study we have improved our earlier proposal,⁸⁾ put forward a new theory based on the molecular orbital method for fragmentation mechanism, and

succeeded in interpreting the fragmentation in several typical cases (CH_3NH_2 , CH_3SH , and CH_3Br).

Experimental

The fragmentation of CH_3X^+ produced by charge-exchange reactions was studied using a perpendicular-type double-mass spectrometer. The details of the apparatus have already been described.¹⁰⁾ In this work, H_2S^+ , C_2H_2^+ , Xe^+ , H^+ , Kr^+ , Ar^+ , Xe^{++} , Ne^+ , and He^+ ions were used as the primary incident ions; they were led into the reaction chamber, where the charge exchange between these ions and CH_3X occurred. The pressure in the reaction chamber was kept below 8×10^{-6} Torr in order to avoid consecutive ion-molecule reactions between the fragment ions and neutral molecules.

Calculation

The eigenvectors of the molecular orbitals of various CH_3X substances were calculated according to the Extended Hückel Molecular Orbital method.⁹⁾ The molecular orbitals to describe these molecules are represented by a linear combination of valence atomic orbitals. The Coulomb integrals of the atomic orbitals, H_{ii} , are shown in Table 1. The resonance integral between the i th and j th atomic orbitals, H_{ij} , was calculated by means of this equation: $H_{ij}=0.5 K(H_{ii}+H_{jj})S_{ij}$, where S_{ij} was the overlap integral and where the value of K was taken to be 1.75, as in Hoffmann's paper.⁹⁾ For the calculation of the overlap integral, Slater μ -values for the valence-shell ns and np atomic orbitals were used as in Mulliken's paper,¹¹⁾ and 4 was taken as the effective quantum number, n^* for bromine.¹¹⁾ The calculation was performed at the Computer Center of Tohoku University.

TABLE 1. H_{ii} VALUES IN THIS CALCULATION

| | H | C | N | O | F | S | Cl | Br | I |
|---------------------|---------------------|---------------------|---------------------|---------------------|---------------------|---------------------|---------------------|---------------------|---------------------|
| $H_{ii}(\text{ns})$ | 13.60 ^{b)} | 18.00 ^{a)} | 24.00 ^{c)} | 24.00 ^{a)} | 31.00 ^{a)} | 16.00 ^{a)} | 18.00 ^{a)} | 27.00 ^{a)} | 24.00 ^{c)} |
| $H_{ii}(\text{np})$ | | 11.26 ^{b)} | 14.49 ^{b)} | 13.62 ^{b)} | 17.42 ^{b)} | 10.36 ^{b)} | 12.97 ^{b)} | 11.81 ^{b)} | 10.45 ^{b)} |

a) A. D. Baker and D. Betteridge, "Photoelectron Spectroscopy," Pergamon Press, London (1972). b) J. Mály and M. Hussonnois, *Theoret. Chim. Acta* (Berl.), **31**, 137 (1973). c) J. A. Bearden and A. F. Burr, *Rev. Mod. Phys.*, **39**, 125 (1967).

* Part I of this series of studies has been published in *Mass Spectroscopy, Japan*, **22**, 233 (1974).

Results and Discussion

Hirota⁵⁾ has proposed the molecular orbital theory to account for the mass spectra resulting from electron impact. According to his theory, the scission probability of the skeletal bonds is proportional to the electron densities of the highest occupied MO at the corresponding bond of the bombarded molecule. However, this theory cannot apply to the following fragmentation processes: (i) the fragmentation to produce the hydrogen-deficient ion from the molecular ion, and (ii) the fragmentation of the molecular ions involving lone-pair electrons. Also, his theory has difficulty in explaining the energy dependence of the fragmentation of the molecular ions as a function of an absorbed energy.⁷⁾

Therefore, we considered the fragmentation mechanism to be as follows:

(1) The bond scission first occurs where the electrons exist densely in the particular occupied MO correlated to the particular ionization.

(2) Process (1) competes with the electron redistribution.

(3) In a higher-energy region, secondary scission also occurs.

Based on Process (1), the primary fragment ions from the molecular ions can be predicted by the main character of the particular MO which is correlated to the particular ionization. For example, if the occupied MO is non-bonding, the ionization caused by the loss of the non-bonding electron should result in the formation of the stable molecular ion. If the occupied MO is C-X bonding, the ionization caused by the loss of

the electron in this orbital should result in the scission of the C-X bond. The absorbed-energy dependence of the fragmentation processes of the molecular ions can be explained by Processes (2) and (3) in addition to Process (1). Although we have obtained the breakdown curves of CH_3X ($\text{X}=\text{NH}_2$, OH , SH , Cl , Br , and I), this paper will deal with the typical fragmentation mechanism of methylamine (CH_3NH_2), methyl mercaptan (CH_3SH), and methyl bromide (CH_3Br).

Methylamine (CH_3NH_2). The electronic configuration and the model employed for this calculation on methylamine are shown in Table 2. The highest occupied MO (HOMO) is non-bonding ($n(\text{N})$) and C-H bonding ($\sigma(\text{C-H})$), because there is a larger population of the eigenvectors in the $\text{N}(2p_z)$, $\text{C}(2p_z)$, and H_1 atomic orbitals. The second occupied MO (SOMO) is C-H bonding ($\pi(\text{CH}_2)$), the third occupied MO (TOMO) is C-H bonding ($\pi(\text{CH}_3)$) and C-N bonding ($\sigma(\text{C-N})$), and the fourth occupied MO (FOMO) is C-N bonding ($\sigma(\text{C-N})$), N-H bonding ($\pi(\text{NH}_2)$), and C-H bonding ($\sigma(\text{C-H})$).

According to Mechanism (1) the mechanism may be considered to be as follows. The ionization caused by the loss of the $\text{N}(2p_z)$ non-bonding electron in HOMO results in the formation of the stable molecular ion, P^+ , while the ionization caused by the loss of the C-H bonding electron in HOMO results in the formation of the $(\text{P-H})^+$ ion, followed by the scission of the C-H bond. The ionization caused by the loss of the electron in SOMO results in the formation of the $(\text{P-}n\text{H})^+$ ion, while the ionization caused by the loss of the electron in TOMO or FOMO results in the formation of the $(\text{P-}n\text{H})^+$, and CH_3^+ or NH_2^+ ions, where $(\text{P-}n\text{H})^+$ ion indicates a hydrogen-deficient species ($(\text{P-H})^+$, $(\text{P-2H})^+$, or $(\text{P-3H})^+$) from the molecular ions. One hydrogen-deficient ion $(\text{P-H})^+$ is considered to have the formula of CH_2NH_2^+ instead of CH_3NH^+ , because the highest occupied MO is C-H bonding (and $n(\text{N})$), while the second occupied MO is also

TABLE 2. CALCULATED IONIZATION POTENTIALS, EIGENVECTORS, MAIN CHARACTER OF MO AND MODEL EMPLOYED FOR CALCULATION ON METHYLAMINE

| Calcd | Ionization potential (eV) | | | |
|----------------------|---------------------------|--------------------|----------------------|---------|
| | 16.17 | 15.55 | 14.19 | 13.44 |
| Obsd ¹²⁾ | 15.6 | 14.5 | 13.2 | 9.7 |
| Eigenvectors | | | | |
| C(2s) | 0.0008 | -0.0184 | 0.0000 | 0.0019 |
| C(2pX) | 0.0000 | -0.0000 | 0.5662 | -0.0000 |
| C(2pY) | -0.3179 | -0.2959 | -0.0000 | 0.0073 |
| C(2pZ) | 0.2723 | -0.3252 | -0.0000 | -0.4262 |
| H ₁ | 0.2973 | -0.1579 | -0.0000 | -0.3936 |
| H ₂ | -0.0089 | 0.2140 | 0.4062 | 0.1766 |
| H ₃ | -0.0089 | 0.2140 | 0.4062 | 0.1766 |
| N(2s) | -0.1419 | 0.0174 | 0.0000 | -0.1105 |
| N(2pX) | -0.0000 | -0.0000 | -0.3518 | 0.0000 |
| N(2pY) | 0.3942 | 0.5620 | -0.0000 | -0.1798 |
| N(2pZ) | 0.4978 | -0.3593 | -0.0000 | 0.7377 |
| H ₄ | 0.1236 | 0.0563 | -0.1620 | 0.0570 |
| H ₅ | 0.1236 | 0.0563 | 0.1620 | 0.0570 |
| Main character | | | | |
| $\sigma(\text{C-N})$ | $\pi(\text{CH}_3)$ | $\pi(\text{CH}_2)$ | $n(\text{N})$ | |
| $\sigma(\text{C-H})$ | $\sigma(\text{C-N})$ | | $\sigma(\text{C-H})$ | |

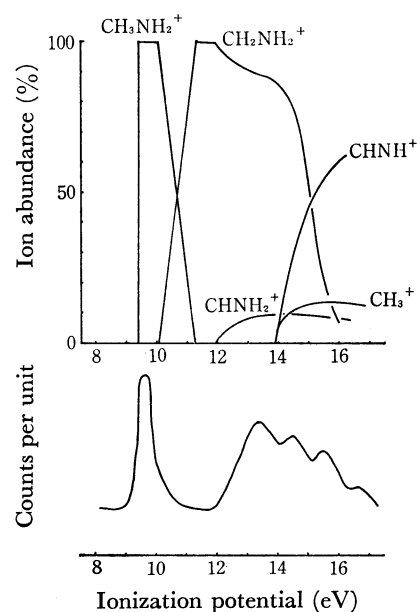
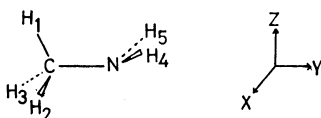


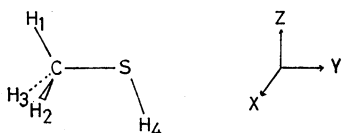
Fig. 1. Comparison of the observed breakdown curve with the photoelectron spectrum¹²⁾ for methylamine.

C-H bonding.

The photoelectron spectrum¹³⁾ and the breakdown curves of methylamine^{14,15)} are shown in Fig. 1. Although the bands (above the second one) of the photoelectron spectrum cannot be discriminated well because of the overlapping, there is an agreement between the appearance potentials of the fragment ions obtained by the charge-exchange and those of the bands in the photoelectron spectrum. That is, the appearance potential of CH_2NH_2^+ and that of CHNH^+ (or CH_3^+) correspond to the ionization potentials of the second and third bands respectively in the photoelectron spectrum. Although the appearance potential of CH_2NH_2^+ does not seem to be equal to the ionization potential of the first band in the photoelectron spectrum, this discrepancy may be ascribed to the dissociation of the vibrationally excited ions. In the region of 10.5–12.0 eV, the cross section for photoelectron emission is small; this phenomenon is also observed in the charge-exchange reaction. The relative abundance of CH_2NH_2^+ obtained by the charge-exchange reactions is large in this region.

TABLE 3. CALCULATED IONIZATION POTENTIALS, EIGENVECTORS, MAIN CHARACTER OF MO AND MODEL EMPLOYED FOR CALCULATION ON METHYL MERCAPTAN

| | Ionization potential (eV) | | |
|---------------------|---------------------------|---------|---------|
| Calcd | 13.89 | 11.52 | 10.38 |
| Obsd ¹³⁾ | 13.67 | 12.08 | 9.44 |
| Eigenvectors | | | |
| C(2s) | -0.0830 | 0.0469 | -0.0000 |
| C(2pX) | 0.0000 | 0.0000 | 0.1514 |
| C(2pY) | -0.5329 | 0.1276 | 0.0000 |
| C(2pZ) | 0.1600 | 0.1332 | 0.0000 |
| H ₁ | 0.1937 | 0.0153 | 0.0000 |
| H ₂ | 0.0319 | -0.0188 | 0.0154 |
| H ₃ | 0.0319 | -0.0188 | -0.0154 |
| S(3s) | -0.0909 | -0.4544 | 0.0000 |
| S(3pX) | 0.0000 | -0.0000 | 0.9881 |
| S(3pY) | 0.4293 | -0.4206 | -0.0000 |
| S(3pZ) | -0.2494 | -0.7056 | 0.0000 |
| H ₄ | 0.2805 | 0.1844 | -0.0000 |
| Main character | | | |
| σ (C-S) | σ (S-H) | n (S) | |
| σ (S-H) | | | |



Methyl Mercaptan (CH_3SH). The electronic configuration and the model employed for this calculation of methyl mercaptan are shown in Table 3. The highest occupied MO is non-bonding ($n(\text{S})$), and the ionization caused by the loss of the non-bonding electron results in the formation of only the stable molecular ion. The second occupied MO is S-H bonding ($\sigma(\text{S-H})$), and the ionization caused by the loss of the S-H bonding electron results in the formation of the $(\text{P-H})^+$ ion.¹⁶⁾ As the third occupied MO is C-S,

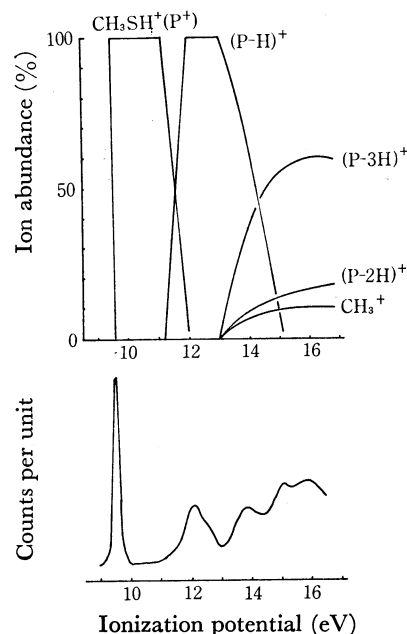


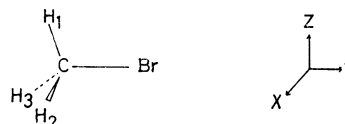
Fig. 2. Comparison of the observed breakdown curve with the photoelectron spectrum¹³⁾ for methyl mercaptan.

C-H, and S-H bonding, the ionization caused by the loss of the electron in this orbital results in the formation of CH_3^+ or SH^+ and of hydrogen-deficient species from the molecular ions.

The photoelectron spectrum¹³⁾ and breakdown curves of methyl mercaptan¹⁷⁾ are shown in Fig. 2. The appearance potential of $(\text{P-H})^+$ is equal to the appearance of the second band of the photoelectron spectrum and the appearance potentials of the $(\text{P-3H})^+$ and CH_3^+

TABLE 4. CALCULATED IONIZATION POTENTIALS, EIGENVECTORS, MAIN CHARACTER OF MO AND MODEL EMPLOYED FOR CALCULATION ON METHYL BROMIDE

| | Ionization potential (eV) | | | | |
|---------------------|---------------------------|-----------------------|---------|---------|---------|
| Calcd | 14.98 | 14.98 | 13.77 | 11.79 | 11.79 |
| Obsd ¹⁸⁾ | 15.85 | 15.14 | 13.52 | 10.85 | 10.53 |
| Eigenvectors | | | | | |
| C(2s) | -0.0000 | -0.0000 | -0.0203 | 0.0000 | 0.0000 |
| C(2pX) | 0.5825 | -0.0000 | 0.0000 | -0.1808 | 0.0000 |
| C(2pY) | 0.0000 | 0.0000 | 0.4079 | -0.0000 | -0.0000 |
| C(2pZ) | 0.0000 | 0.5825 | -0.0000 | 0.0000 | 0.1808 |
| H ₁ | 0.0000 | 0.4848 | 0.0448 | 0.0000 | 0.0147 |
| H ₂ | 0.4198 | -0.2424 | 0.0448 | -0.0127 | -0.0073 |
| H ₃ | -0.4198 | -0.2424 | 0.0448 | 0.0127 | -0.0073 |
| Br(4s) | -0.0000 | -0.0000 | -0.1946 | -0.0000 | -0.0000 |
| Br(4pX) | 0.1251 | -0.0000 | 0.0000 | 0.9833 | -0.0001 |
| Br(4pY) | -0.0000 | -0.0000 | -0.7324 | -0.0000 | -0.0000 |
| Br(4pZ) | 0.0000 | 0.1251 | -0.0000 | -0.0001 | -0.9833 |
| Main character | | | | | |
| $\pi(\text{CH}_2)$ | $\pi(\text{CH}_3)$ | $\sigma(\text{C-Br})$ | n(Br) | n(Br) | |



ions are equal to that of the third band. This means that the production of the fragment ions is correlated to the electronic configuration of the molecule. It is clearly shown in Fig. 2 that the stable molecular ion is obtained after the ionization caused by the loss of the electron in the highest occupied MO, the $(\text{P-H})^+$ ion is obtained after that in the second occupied MO, and the $(\text{P-3H})^+$ and CH_3^+ ions are obtained after that in the third occupied MO. These results are in good accordance with our theoretical consideration for the production of the fragment ions.

Methyl Bromide (CH_3Br). The electronic configuration and the model employed for this calculation of methyl bromide are shown in Table 4. As may clearly be seen from the table, the highest occupied MO (which is degenerate) is non-bonding ($n(\text{Br})$), and the ionization caused by the loss of the non-bonding electron results in the formation of a stable molecular ion. The second occupied MO is C-Br bonding ($\sigma(\text{C-Br})$), and the ionization caused by the loss of the C-Br bonding electron results in the formation of CH_3^+ or Br^+ . The third occupied MO is C-H bonding, and the ionization of the C-H bonding electron results in the formation of the CH_2Br^+ ion.

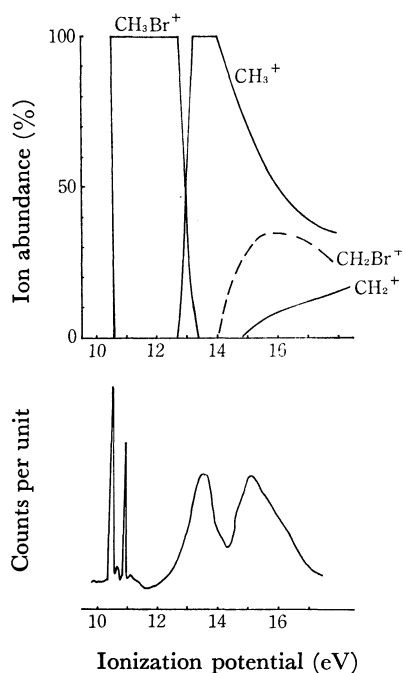


Fig. 3. Comparison of the observed breakdown curve with the photoelectron spectrum¹⁸⁾ for methyl bromide.

The photoelectron spectrum¹⁹⁾ and the breakdown curves of CH_3Br ²⁰⁾ are shown in Fig. 3. The appearance potential of CH_3^+ is equal to that of the second band of the photoelectron spectrum, while the appearance potential of CH_2Br^+ is equal to that of the third band. Accordingly, these results are also in good accordance with our theoretical consideration for the production of the fragment ions.

The energy dependence of the scission probability of the C-X bond in various CH_3X^+ substances ($\text{X}=\text{NH}_2$, OH, SH, Cl, Br, and I) obtained by the charge-exchange

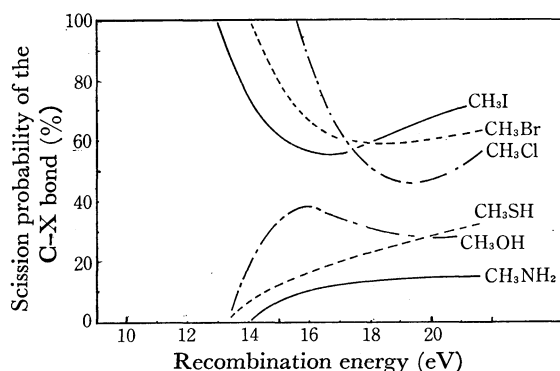


Fig. 4. The observed scission probabilities of the C-X bond in various CH_3X as a function of recombination energy.

TABLE 5. MAIN CHARACTER IN THE HIGHEST, SECOND, AND THIRD OCCUPIED MOLECULAR ORBITALS ON VARIOUS CH_3X

| | Group A | | |
|---------|-----------------------|-----------------------|-----------------------|
| | Cl | Br | I |
| Highest | $n(\text{Cl})^a)$ | $n(\text{Br})^a)$ | $n(\text{I})^a)$ |
| Second | $\sigma(\text{C-Cl})$ | $\sigma(\text{C-Br})$ | $\sigma(\text{C-I})$ |
| Third | $\pi(\text{CH}_3)^a)$ | $\pi(\text{CH}_3)^a)$ | $\pi(\text{CH}_3)^a)$ |

| | Group B | | |
|---------|--|--|--|
| | NH_2 | OH | SH |
| Highest | $n(\text{N}), \pi(\text{CH}_3)$ | $n(\text{O})$ | $n(\text{S})$ |
| Second | $\pi(\text{CH}_2)$ | $\pi(\text{CH}_3)$ | $\sigma(\text{S-H})$ |
| Third | $\sigma(\text{C-N}), \pi(\text{CH}_3)$ | $\sigma(\text{C-O}), \sigma(\text{C-H})$ | $\sigma(\text{C-S}), \sigma(\text{S-H})$ |

a) Orbital is degenerate

reactions is shown in Fig. 4. The sum of the abundance of the CH_3^+ and X^+ (produced by the ionization caused by the loss of the C-X bonding electron) was plotted as a function of the absorbed energy of CH_3X . The main characteristics of the highest, second, and third occupied MO's on various CH_3X are shown in Table 5. There are outstanding differences in the main characters in the second and third occupied MO's between Groups A and B. These differences are directly related to the fragmentation processes between the two groups (as is shown in Figs 1. (or 2) and 3, or 4). Moreover, it may be suggested that the order of the scission probability of the C-X bond shown in Fig. 4 corresponds to that of the bond population ($C_i C_j S_{ij}$, where C_i and C_j are the eigenvectors of the i th and j th atomic orbitals, and where S_{ij} is the overlap integral between them) in the second or third occupied MO.²¹⁾

From these results it is obvious that the bond scission first occurs where the electrons exist densely in the particular occupied MO correlated to the particular ionization [Mechanism (1)]. The scission probability can be well predicted by means of the main characteristics and the bond populations of various occupied MO's (which fit the ionization energy) in the cases of simple compounds of CH_3X . Considerations of Mechanism (2), the redistribution of electrons, may become more significant for the more complicated systems, such as $\text{C}_2\text{H}_5\text{X}$, $\text{C}_3\text{H}_7\text{X}$, and $\text{C}_4\text{H}_9\text{X}$.²²⁾ This subject will be discussed in succeeding papers,

References

- 1) H. M. Rosenstock, M. B. Wallenstein, A. L. Wahrhaftig, and H. Eyring, *Proc. Natl. Acad. Sci., U.S.*, **38**, 667 (1952).
- 2) M. L. Vestal, *J. Chem. Phys.*, **43**, 1356 (1965).
- 3) E. Lindholm, "Ion-Molecule Reactions," Vol. 2, ed. by Franklin, Plenum Press, New York (1972), p. 457.
- 4) H. M. Rosenstock, J. T. Larkins, and J. A. Walker, *Int. J. Mass Spectrom. Ion Phys.*, **4**, 309 (1973).
- 5) for example; K. Hirota, *Nippon Kagaku Zasshi*, **91**, 585 (1970).
- 6) J. C. Lorquet, *Mol. Phys.*, **9**, 101 (1965).
- 7) S. Ikuta, K. Yoshihara, and T. Shiokawa, *This Bulletin*, **46**, 3648 (1973).
- 8) S. Ikuta, K. Yoshihara, and T. Shiokawa, *Mass Spectroscopy, Japan*, **22**, 233 (1974).
- 9) R. Hoffmann, *J. Chem. Phys.*, **39**, 1397 (1963).
- 10) T. Shiokawa, K. Yoshihara, M. Yagi, T. Omori, H. Kaji, M. Hiraga, T. Nagatani, and Y. Takita, *Mass Spectroscopy, Japan*, **18**, 1230 (1970).
- 11) R. S. Mulliken, C. A. Rieke, D. Orloff, and H. Orloff, *J. Chem. Phys.*, **17**, 1248 (1949).
- 12) A. B. Cornford, D. C. Frost, F. G. Herring, and C. A. McDowell, *Can. J. Chem.*, **49**, 1135 (1971).
- 13) H. Ogata, H. Onizuka, Y. Nihei, and H. Kamada, *This Bulletin*, **46**, 3026 (1973).
- 14) H. Sjögren, *Arkiv Fysik*, **29**, 565 (1965).
- 15) T. Nagatani, K. Yoshihara, and T. Shiokawa, *This Bulletin*, **46**, 3036 (1973).
- 16) This (P-H)⁺ ion is considered to have a formula of CH₃S⁺ because ionization of the electron in SOMO which is S-H bonding will produce this ion by the scission of the S-H bond.
- 17) K. Yoshihara, M. Kobayashi, S. Ikuta, and T. Shiokawa, *This Bulletin*, in press.
- 18) J. L. Ragle, I. A. Stenhouse, D. C. Frost, and C. A. McDowell, *J. Chem. Phys.*, **53**, 178 (1970).
- 19) D. W. Turner, "Molecular Photoelectron Spectroscopy", John Wiley & Sons, New York, N. Y. (1969).
- 20) S. Ikuta, K. Yoshikawa, and T. Shiokawa, *Mass Spectroscopy, Japan*, to be published.
- 21) The values of the bond population of the C-X bond in the second or third occupied molecular orbitals are as follows.
 CH₃-NH₂: 0.052, CH₃-OH: 0.057, CH₃-SH: 0.110,
 CH₃-Cl: 0.125, CH₃-Br: 0.144, CH₃-I: 0.143
- The order of the scission probability of the C-X bond shows reverse tendency for CH₃OH and CH₃SH concerning the calculated and observed ones (see Fig. 4). This may be influenced by the degree of elimination of H₂O and/or H₂S from the molecular ions.
- 22) S. Ikuta, K. Yoshihara, and T. Shiokawa, *This Bulletin*, to be published.